16th Australasian Fluid Mechanics Conference
Crown Plaza, Gold Coast, Australia
2-7 December 2007

Flow-Structure Interaction in the Upper Airway: Motions of a Cantilevered Flexible Plate in Channel Flow with Flexible Walls

J. Wang, G.A. Tetlow and A.D. Lucey

Fluid Dynamics Research Group
Curtin University of Technology, Western Australia, 6845 AUSTRALIA

Abstract

The present work seeks to elucidate the flow-structure dynamics of the upper airway so that improved clinical strategies for the alleviation of snoring and sleep apnoea can be developed and applied on an evidence basis. Analogue computational modelling, appropriately related to the anatomically correct system, is used. Hitherto, such modelling has been confined to flow in a rigid-channel to study flutter of the soft palate. Clinical evidence suggests that apneic events can involve combined motions and interactions of the soft palate and flexible walls of the pharynx. We model a flexible cantilevered plate (the soft-palate) mounted in a channel of square cross-section (the pharynx), the downstream side walls of which are flexible to capture deformation in airway collapse. Upstream of the flexible plate is a rigid plate (the hard palate) that spans the channel to permit airflow to be drawn from two inlets (oral and nasal). The commercial FSI software ADINA is used to construct the model and undertake the three-dimensional investigation. Results show that motions of the soft-palate have little effect on the deformation of the side walls. However, the amplitude and frequency of soft-palate vibrations are found to be strongly dependent upon side-wall stiffness and, hence, dynamics.

Introduction

The present work is motivated by the need to understand the complex fluid-structure interactions that occur in the upper airway. The coupled dynamics of airflow, soft-palate vibrations and motion of the airway walls (the pharynx) in humans underpin snoring and the more serious condition of sleep apnoea whereby the airway undergoes total closure. A complete understanding of the mechanical causes of these conditions is as yet unavailable. Endoscopic observations suggest that snoring noises originate from oscillations of the soft palate that separates oral and nasal inlets while airway collapse occurs in the oropharynx near the tip, or just downstream, of the soft palate. Clinical observations suggest that soft-palate motions are implicated in some 30% of apneic events. Figure 1 identifies these anatomical landmarks on a reconstructed geometry of the upper airway that we obtained in [7] using catheter-based optical tomography in combination with CT-scans.

The dynamics of a cantilevered flexible plate in channel flow as a model for the mechanics of snoring has received much attention; for example, see [1,2,4,6]. Such studies focus upon the stability characteristics of the flexible plate, showing that beyond a critical flow speed or Reynolds number, the plate succumbs to flutter instability. However all such studies have been two-dimensional and assumed rigid channel walls. The study of flexible tubes through which a fluid is flowing has received vast attention for the rich dynamics that this system contains; for two excellent reviews of theoretical and experimental work, see [5] and [3].

In this paper we combine key features of the two distinct strands of study described above; the pharynx is a flexible tube in which is mounted a cantilevered flexible, the soft-palate. Each flexible component of the system has its own dynamics and these will be coupled through the fluid flow. Our goal herein is to take the first steps towards establishing an understanding of this complex flow-structure system.

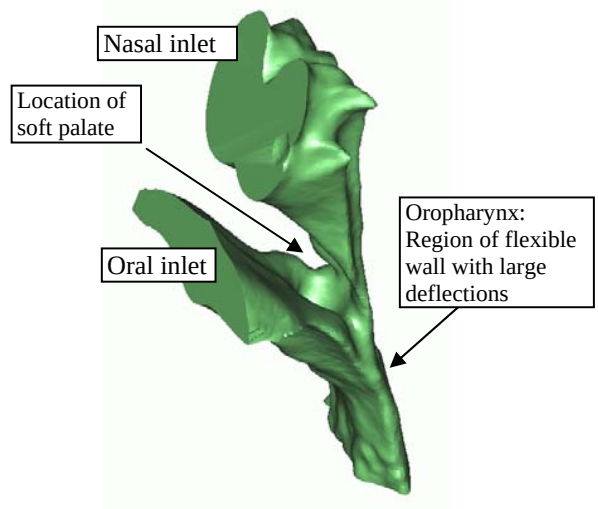

Figure 1. Anatomically measured upper airway model; from [7]

Analogue Computational Modelling

The analogue computational model is shown in Fig. 2. It is topologically mapped from the anatomically correct layout of Fig. 1 but is radically simpler to permit the extraction of only the core system dynamics. It comprises four rigid parts, one fluid block, a flexible plate (soft palate) and two flexible side walls.

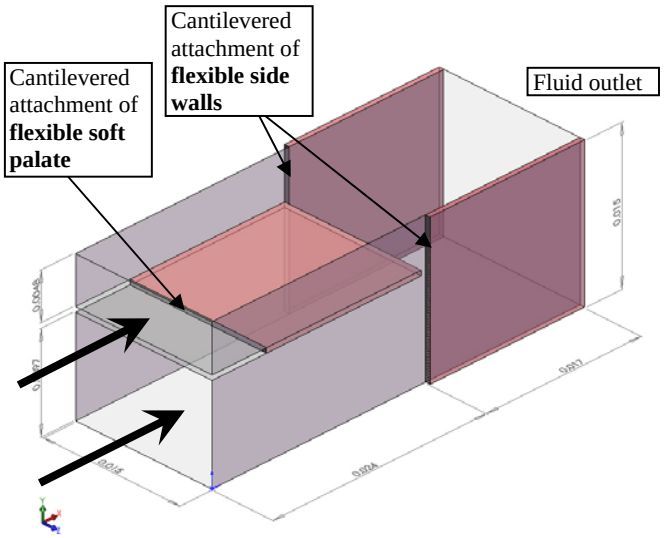

Figure 2. Analogue computational model; the arrows indicate inhalation through upper (nasal) and lower (oral) airways.

The model permits airway closure only through the motion of the cantilevered flexible side walls that are allowed to slide freely (without leakage) past the upper and lower walls. The rigid upper wall represents the tongue that, although flexible, is stiff relative to the side walls of the oropharynx. The lower wall can be assumed rigid because the pharynx abuts the spine. The soft palate and two flexible side walls have identical dimensions (17 x 15 x 0.5 mm) with material density 1000 kg/m^3 and Poisson ratio 0.33. The cross-section of the wholly rigid channel enclosing the upstream hard and soft palates has both width and height of 15 mm. Within this section, the hard and soft palate are offset to give lower and upper channel heights of 9.7 mm and 4.8 mm respectively (with palate thicknesses being 0.5 mm). This asymmetry represents the different calibres of the oral and nasal airways that are separated by the palate. The lengths of the hard and soft palates are 9 mm and 17 mm respectively and the overall length of the system is 41 mm. All of these dimensions have been chosen to be broadly representative of an adult. There is a three-sided fluid-structure interaction (FSI) boundary for the soft palate (upper and lower surfaces, and tip side surface) while there is just one interior FSI boundary for each side wall. Unsteady three-dimensional laminar flow is assumed, modelled by the Navier-Stokes and Continuity equations. The airflow is driven by a pressure loading, ΔP , applied across the length of the system. The external pressure is taken to be that of the inlet side.

Numerical Investigation

The commercial FSI software ADINA R&D, a fully coupled finite-element solver, is used for all of the investigations reported herein. Implicit schemes have been selected to predict the motion of all of the flexible surfaces and a transient analysis for the fluid dynamics. A series of numerical experiments is performed for a range of soft palate and side-wall material properties. A single applied pressure load of $\Delta P = 0.28$ Pa is used throughout and the properties of air are those at 20^0 C. The load is applied as a linear ramp function for the first 50 time steps of a numerical experiment to reach full load at 1 s. For the next 9 seconds, a further 150 time steps of size 0.06 s, at constant full load, are computed to predict the motion; thus, all time series run for 10 s. A high-resolution preliminary simulation was first carried using 250,000 fluid tetrahedral elements and 30,000 solid brick elements. Since displacements of soft-palate tip were found to be small, adaptive meshing was then not needed, and thus a simpler all-brick element model could be deployed. Moreover, we were able to reduce the level of discretisation down to 40,000 fluid plus 3,000 solid brick elements with just a 3% reduction to the accuracy of the maximum deflection of the soft palate.

A typical result is shown schematically in Fig. 3. The soft palate is seen to deform upwards (y-displacement) and in the quantitative results that follow we track the position of Node A as being representative of soft-palate (maximum) deflection. This is reasonable since the deformation of the soft palate is overwhelmingly planar. Correspondingly, (z-displacement) deformation of the side-walls is represented by Node B, at mid-channel height. In this case there is non-negligible variation in the vertical direction so choosing the mid-point records the maximum displacement. For this preliminary study, chosen to use a combination of pressure loading, channel dimensions and soft-palate properties that yields stable oscillatory behaviour, i.e. the mean flow speeds and Reynolds number are beneath those that would cause soft-palate flutter.

Results

First, we assess the effect of soft-palate motion on side-wall response. Next we reverse the investigation to quantify the effect of side-wall motion on soft-palate behaviour. Finally, we combine these results in a simple non-dimensional framework. Throughout we vary motion of the flexible components by changing their elastic moduli while keeping all other parameters, both geometric and material, unchanged.

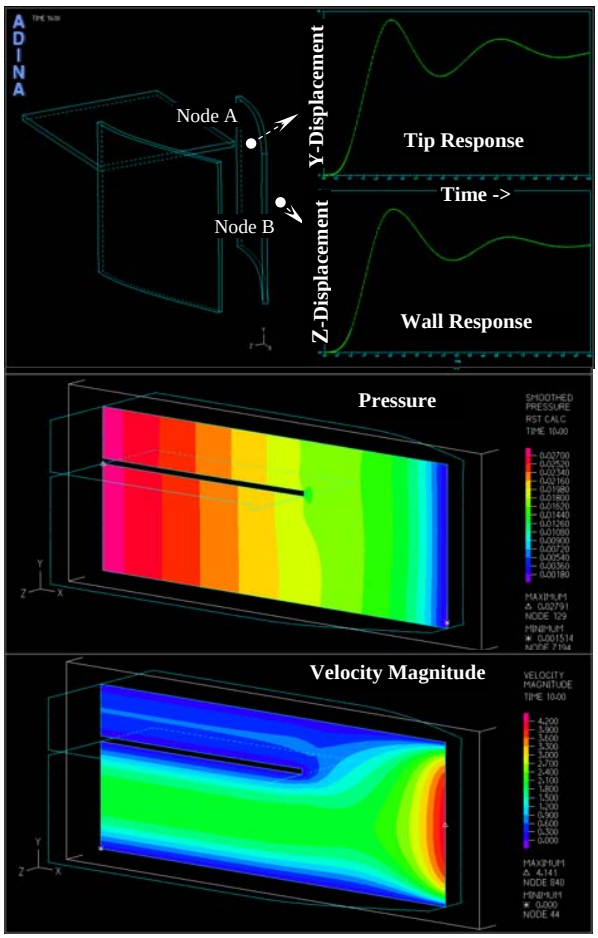

Figure 3. Illustrative simulation of the flow-structure interaction; (a) generation of a 10-second time series and centreline flow at final equilibrium, (b) pressure contours, (c) velocity magnitude.

First, we assess the effect of soft-palate motion on side-wall response. Next we reverse the investigation to quantify the effect of side-wall motion on soft-palate behaviour. Finally, we combine these results in a simple non-dimensional framework. Throughout we vary motion of the flexible components by changing their elastic moduli while keeping all other parameters, both geometric and material, unchanged.

The effect of soft-palate motion on side-wall response

Figures 4 and 5 show time series for the palate-tip and side-walls for the two cases of side-wall elastic modulus (E_w) being 200 and 2800 N/m^2 respectively. For each case a range of soft-palate elastic modulus (E_P) is used to vary the amplitude of its motion.

It is seen throughout that the soft-palate deflects upwards into the narrower channel as shown through the independent methods of [6] while the side-walls move inwards to create a partial closure of the channel at its downstream end. Soft-palate oscillations are seen to be attenuated in these sub-critical conditions. The infinite-time result has the system arriving at a new static equilibrium position. The soft palate always comes to rest deflected into the upper, narrower, channel because there is greater flow-speed and mass flux through the lower, wider,

channel that has lower resistance; see Figs. 3b and 3c. At the soft-palate tip the upper and lower channel-flows combine. A separated shear layer exists that must deflect towards the top rigid wall like the flow over a backward facing step in the extreme case of infinite upper-channel resistance. The resulting curvature of the isobars in the lower channel relative to those in the upper channel then produces a net upwards force that deflects the soft-palate. As seen in Figs. 4 and 5, the lower the value of the soft-palate stiffness, the greater is its deflection.

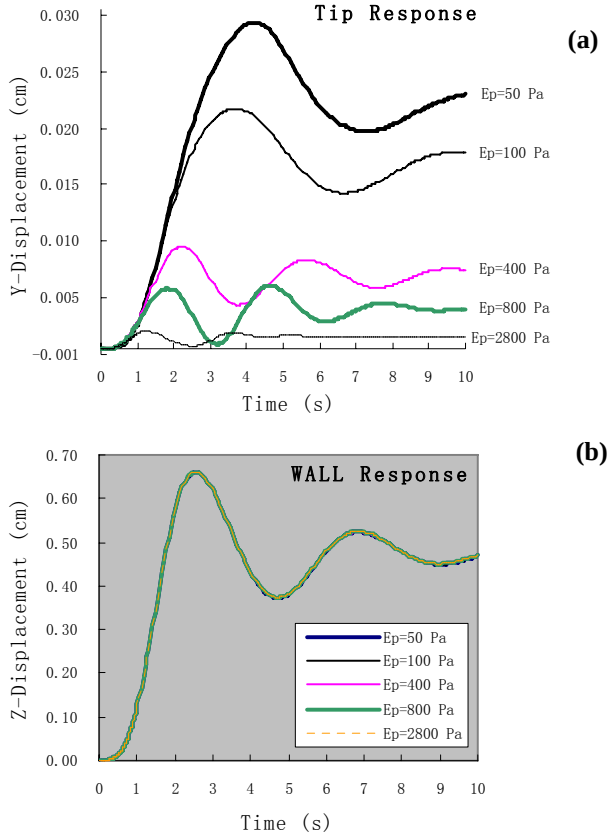

Figure 4. Time series of (a) soft-palate tip, and (b) side-wall mid-point motion for a flexible side-wall with E_w =200 N/m^2.

Figures 4a and 5a clearly show that changing E_P strongly influences the soft-palate deflection. However, corresponding changes in E_W generate only a small change in side-wall deflection as evidenced by contrasting Figs. 4b and 5b. Equally evident in these latter figures is that the magnitude of the soft-palate deflection has virtually no effect on the side-wall deformation. To further confirm the insensitivity of side-wall to soft-plate deflection we have artificially added uniform loads to the soft-palate, for just the first 0.5 s, that increase the amplitude of its oscillations. As already seen in Figs. 4a and 5a the soft-palate deflection ultimately asymptotes to a static deformed state. Prior to this, very large amplitudes of oscillation are observed. and yet these motions have very little effect on the side-wall motion. In fact, an increase to the soft-palate amplitude by a factor of 28 results in only a maximum change of 2.8% in the amplitude of side-wall movement. This signals the insensitivity of side-wall motion to the dynamics of the soft plate.

The effect of side-wall motion on soft-palate response

The motion of the soft-palate tip has been recorded over a range of side-wall stiffness for a number of cases of soft-palate stiffness. Figures 6a and 6b respectively show the cases E_P=200 and 800N/m^2. A broad contrast of the two figures (and noting the scales of the vertical axes) shows that soft-palate deformation decreases with increases to E_P as already seen in Figs. 4a and 5a. Of greater interest in these figures is that both the transient oscillations of the soft palate and amplitude of the final static equilibrium achieved are strongly dependent upon E_W and thus the deformation of the side walls. In most cases, the higher the deformation of the side walls – or extent of channel closure – then the more the soft-palate deforms. However, in Fig. 6a it is an intermediate value of E_W that yields the highest transient amplitude of the soft-palate; this suggests some form of resonance between the motions of the different flexible surfaces. We also remark that for stiffer soft-palates the transient behaviour can feature incursions of the soft palate into the lower channel.

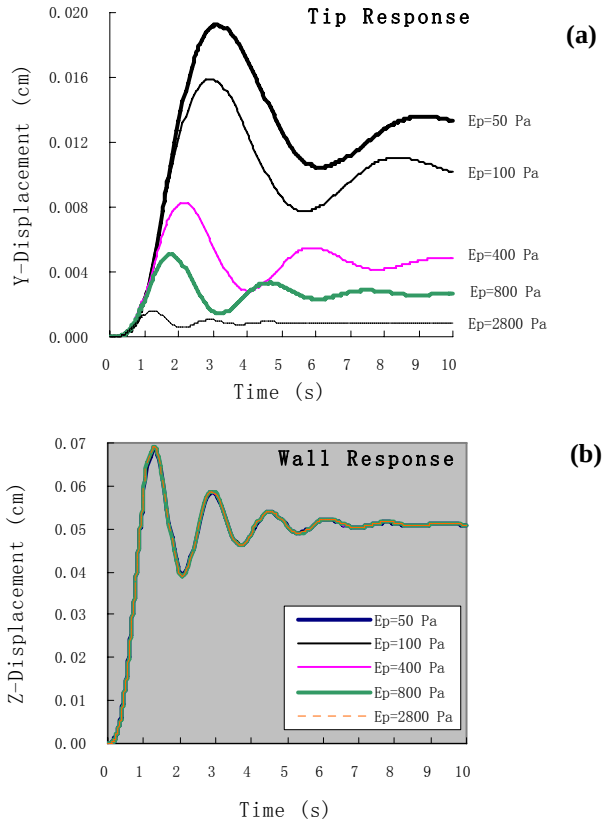

Figure 5. Time series of (a) soft-palate tip, and (b) side-wall mid-point motion for a flexible side-wall with E_w =2800 N/m^2.

Characterisation of the coupled mechanics

Since side-wall behaviour has been shown to be insensitive to soft-palate motions, its behaviour may be reasonably predicted by assuming a rigid soft palate. By contrast, soft-palate behaviour is strongly dependent upon both soft-palate and side-wall material properties. Three features of soft-palate response, drawn from Fig. 6 (and further results for other values of E_P) are used to characterise this behaviour: (a) the final static-equilibrium tip deflection, (b) the peak amplitude [relative to the value of (a)] in the transient phase, and (c) the frequency of its oscillations in the transient phase. Displacements (a) and (b) are non-dimensionalised based on in-vacuo plate mechanics for which the peak deflection due to a distributed load is ($3\,\Delta P\,L^4/2E_Ph^3$) where L and h are the plate length and thickness respectively. We use ΔP on the assumption that the transmural fluid loading is directly related to the applied streamwise pressure drop across the entire channel. For a time-scale to non-dimensionalise the frequency, we use $k/(E_p)^{0.5}$ with k=1 for convenience. Figures 7a, 7b and 7c then show the variation of the above three features for

different values of E_P. While clear trends emerge, there is not total collapse of the data. This suggests that a more complex scheme is required that accounts for both solid and fluid parameters in the system. This is further suggested by a type of frequency lock-in when $E_W/E_P=1$ in Fig.7c and recalling that the only means of coupling is through the fluid medium.

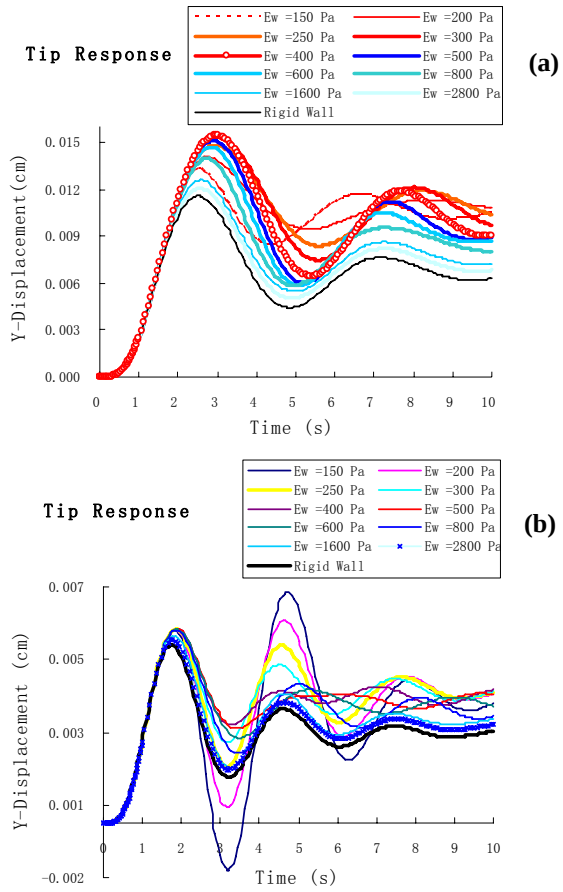

Figure 6. Effect of side-wall stiffness on tip motion for two different soft-palates: (a) E_P=200, and (b) E_P=800 N/m^2.

Conclusions

An analogue computational model of the upper airway, combining soft-palate and flexible side-walls coupled through airflow has been developed and used to explore the interaction between these three dynamical elements. It is shown that the side-wall response to the airflow is largely independent of motions of the upstream soft palate. Conversely, the motion and final equilibrium of the soft-palate is strongly dependent upon side-wall flexibility and, hence, deformation. This dependence has been mapped for the single geometric configuration adopted in this paper. Further work will seek to quantify the effect of transients on upper-airway stability in such cases as, one inlet channel closed (breathing through nose only) and the transition from inhalation to exhalation.

References

[1] Aurégan, Y. & Depollier, C.,Snoring: Linear stability analysis and in-vitro experiments. *J. Sound Vib.*, **188**, 1995, 39-54.

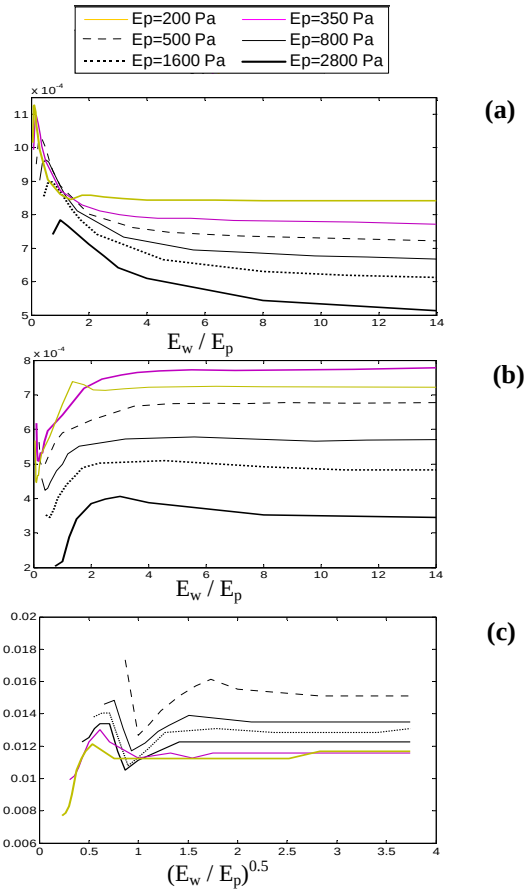

Figure 7. Variation of non-dimensionalised soft-palate motion with side-wall stiffness: (a) final tip deflection, (b) peak amplitude of oscillation, and (c) frequency of oscillation.

[2] Balint, T.S. & Lucey A.D., Instability of a cantilevered flexible plate in viscous two-dimensional channel flow. *J. Fluids Struct.*, **20**, 2005, 893-912.

[3] Bertram, C.D.,Experimental Studies of Collapsible Tubes. In *Flow Past Highly Compliant Boundaries and in Collapsible Tubes*, eds. PW Carpenter & TJ Pedley, Kluver, 2003, 51-65

[4] Guo, C.Q. & Paidoussis, M.P. Stability of Rectangular Plates with Free Side-Edges in Two-Dimensional Inviscid Channel Flow. *J. Appl. Mech.* **67**, 2000, 171-176.

[5] Heil, M. & Jensen, O.E. (2003) Flows in deformable tubes and channels. In *Flow Past Highly Compliant Boundaries and in Collapsible Tubes*, eds. PW Carpenter & TJ Pedley, Kluver, 2003, 15-49, Kluwer.

[6] Tetlow, G.A., Lucey, A.D. & Balint, T.S. Instability of a cantilevered flexible plate in viscous channel flow driven by constant pressure drop. 2006, ASME Paper PVP2006-ICPVT11-93943.

[7] Wang, J., Tetlow. G.A., Lucey, A.D., Armstrong, J.J., Leigh, M.S., Paduch, A., Sampson, D.D, Walsh, J.H., Eastwood, P.R., Hillman, D.R., Harrison, S.,Dynamics of the human upper airway: On the development of a three-dimensional computational model. In IFMBE Proc. (CD) **14** (World Congress on Medical Physics and Biomechanical Engineering, 2006